IEEE Access
Multidisciplinary | Rapid Review | Open Access Journal

Received August 15, 2019, accepted August 24, 2019, date of publication August 30, 2019, date of current version September 12, 2019.

Digital Object Identifier 10.1109/ACCESS.2019.2938256

Aerial Small Cells Using Coordinated Multiple UAVs: An Energy Efficiency Optimization Perspective

CHENGXIAO LIU[1], WEI FENG[1], (Senior Member, IEEE), JUE WANG[2], (Member, IEEE), YUNFEI CHEN[3], (Senior Member, IEEE), AND NING GE[1], (Member, IEEE)

[1]Beijing National Research Center for Information Science and Technology, Tsinghua University, Beijing 100084, China
[2]Nantong Research Institute for Advanced Communication Technologies, Nantong University, Nantong 226019, China
[3]School of Engineering, University of Warwick, Coventry CV4 7AL, U.K.

Corresponding author: Wei Feng (fengwei@tsinghua.edu.cn)

This work was supported in part by the Beijing Natural Science Foundation under Grant L172041, in part by the National Natural Science Foundation of China under Grant 61771286, Grant 61701457, Grant 61771264, and Grant 91638205, and in part by the Beijing Innovation Center for Future Chip.

ABSTRACT Recently, unmanned aerial vehicle (UAV) communications have attracted great research interest. Due to the limited on-board energy, the optimization of energy efficiency (EE) is critical for UAV communications. In this paper, we propose an EE maximization scheme for UAV swarm-enabled small cell networks using large-scale channel state information at the transmitter (CSIT). The proposed scheme provides an agile coordination strategy for the UAVs in a swarm under energy constraints. We first formulate the EE maximization problem, where the objective function is defined as the ratio of the ergodic total data size to the total energy consumption. After that, an accurate approximation is derived to remove the intractable expectation operator in the objective function. As the newly formulated problem is non-convex, we decompose it into two subproblems to optimize the transmit power and the hovering time in an iterative way. Further by leveraging the max-min and linear optimization tools, both subproblems are efficiently solved. Simulation results demonstrate the superiority of our EE maximization scheme.

INDEX TERMS Coordinated power allocation, energy efficiency, small cell, time scheduling, unmanned aerial vehicle.

I. INTRODUCTION

Nowadays, unmanned aerial vehicle (UAV) communications have attracted great research interest [1], [2]. Deployed as mobile aerial base stations (BSs), the UAVs can adapt to the increasing demand for mobile terminals (MTs) in a vast coverage area, whereas the coverage area of conventional terrestrial BSs is usually limited [2], [3]. Therefore, UAV communications have been regarded as promising techniques for future networks [1]–[5].

In practice, the endurance of UAVs is an essential issue to be addressed in the design of UAV communication networks [1], [2]. As most rotary-wing UAVs are small-sized and battery-powered [1], the on-board energy of UAVs, including the propulsion energy and the communication energy, is extremely limited [2], [6]. Hence, the optimization of energy efficiency (EE) is critical for UAV-enabled networks, where a number of related works have been conducted [7]–[12]. Zeng *et al.* optimized the EE of UAVs in [7], considering the energy consumption of UAV propulsion. Mozaffari *et al.* maximized the EE considering the total uplink power constraint of the Internet of Things (IoT) devices in [8]. Liu *et al.* proposed a novel UAV control strategy in [9], which maximized the EE through deep reinforcement learning. Song *et al.* maximized the EE of multi-antenna UAV-enabled mobile relay in [10], which discussed the trade-off between the throughput and propulsion energy consumption. Zhou *et al.* optimized the EE of UAVs for industrial internet in [11], which proposed a UAV control strategy in smart grid. Ghorbel *et al.* minimized the energy consumption of UAVs to optimize the EE in [12], which used the cognitive radio techniques.

The limited energy of a single UAV motivates the use of UAV swarm in networks [13]–[20]. The authors of [13]

The associate editor coordinating the review of this article and approving it for publication was Chi-Tsun Cheng.

proposed a scheme to cover a given area with the minimum number of UAVs. In [14], an energy-efficient multi-UAV coverage algorithm was proposed based on the game-theoretic framework. In [15], a UAV swarm path planning algorithm was proposed considering the propulsion energy consumption of UAVs. The authors of [16] optimized the trajectory of a UAV swarm to serve users in a network using the shortest time. In [17], a distributed UAV flocking model was proposed based on the positioning and communication techniques. In [18], a layered UAV swarm network structure was proposed using a low-latency routing algorithm. The authors of [19] optimized the spectrum efficiency and EE jointly through trajectory planning. In [20], the positioning of UAVs was optimized using deep Q-learning technique in dynamic UAV swarm networks. To further improve the performance of UAV swarm-enabled networks, aerial small cells were considered, where the UAVs work as small cells to provide high-speed services in a coordinated manner [21]–[23]. In [21], a dynamic path planning algorithm was proposed for UAV-based aerial small cells. The authors of [22] proposed an energy-aware 3D deployment algorithm for UAV swarm-based aerial small cells. In [23], the coverage of multiple UAVs was maximized in the presence of co-channel interference.

Due to the increasing service demand, the communication energy consumption of UAVs becomes considerable, which should be taken into account in the system design [15], [24], [25]. The authors of [15] considered the communication energy consumption in UAV path planning schemes to maximize the sum rate. In [24], the communication energy was minimized by scheduling the hovering time of UAVs. In [25], we jointly optimized the communication energy and hovering time to maximize the total data size for UAV-aided IoT communications. However, the optimization of EE for UAV-swarm enabled small cell networks has not been addressed in any of the previous works.

In this paper, we address the EE maximization issue for UAV swarm-enabled small cell networks. Motivated by practical constraints, we assume only the slowly-varying large-scale channel state information (CSI) is available for optimization. In contrast, a simplified free-space path-loss channel model was assumed in most previous works [15], [16], [18], [24]. While adopting the simplified channel model can facilitate the mathematical analysis, it deviates from the realistic UAV channel conditions, which may cause severe performance degradation [25]. To characterize a realistic communication environment, a composite channel model was considered in the design of UAV swarm-enabled small cell networks [25], [26]. This model considers both the line-of-sight (LOS) and non-line-of-sight (NLOS) channel elements, so that it is more practical than the simplified models. Concretely, this model includes both the large-scale channel fading, i.e. the position-related slowly-varying CSI, and the small-scale channel fading, i.e. the stochastic fast-varying CSI. It is worth noting that the small-scale CSI at the transmitter (CSIT) is in general not available prior to the UAV flight due to its inherent unpredictability. However, the large-scale CSIT can be acquired [25], [27], thanks to the fact that both the pre-scheduled trajectory of UAVs and the locations of MTs can be known prior to the flight [15], [16]. The main contributions of this paper are summarized as follows.

- We formulate an EE maximization problem for UAV swarm-enabled small cell networks with large-scale CSIT, where the objective is to maximize the ratio of the ergodic total data size to the total energy consumption. We propose an accurate approximation using a newly derived analytic function to remove the intractable expectation operator in the objective function to simplify the problem.
- We further decompose the simplified EE maximization problem into two subproblems. One subproblem is to find the optimal coordinated power allocation strategy, which is a nonlinear fractional optimization problem and known to be non-convex. An iterative algorithm is proposed to solve this subproblem. The other subproblem is to find the optimal hovering time scheduling strategy, which is a linear fractional optimization problem and can be efficiently solved after a series of reformulations.
- Based on the solutions to the two subproblems, i.e. the power allocation strategy and the hovering time scheduling strategy, we propose an iterative algorithm to solve the original EE maximization problem with guaranteed convergence. Simulation results demonstrate the superiority of the proposed algorithm.

The rest of this paper is organized as follows. In Section II, we introduce the system model and the channel model, where the formulation of the proposed EE maximization problem is also introduced. The solution to the EE maximization problem is given in Section III. Section IV presents the simulation results and discussions. Section V gives the conclusion.

II. SYSTEM MODEL

We consider a general UAV swarm-enabled small cell network, as shown in Fig. 1. To control the cost of UAV communications [1], we assume the swarm consists of K single-antenna UAVs. Each UAV acts as an aerial small cell BS, and all UAVs in the swarm serve N MTs in a coordinated manner. Specifically, the UAV swarm works in an energy-efficient *hover-to-transmit* mode [15], [16], which means that the aerial small cells will hover at the MT for some time to serve it and then fly to the next MT. Without loss of generality, each MT is assumed to have M receive antennas, so that the received signal of the n-th MT can be expressed as

$$\mathbf{y}_n = \mathbf{H}_n \mathbf{x}_n + \mathbf{q}_n, \quad n = 1 \sim N \tag{1}$$

where $\mathbf{H}_n \in \mathbb{C}^{M \times K}$ denotes the channel matrix, $\mathbf{x}_n$ is the transmit signal of UAVs and $\mathbf{q}_n$ denotes the Additive White Gaussian Noise following $CN(\mathbf{0}_M, \sigma^2 \mathbf{I}_M)$, where $\mathbf{0}_M \in \mathbb{C}^M$ and $\mathbf{I}_M \in \mathbb{C}^{M \times M}$ are the all-zero vector and the identity matrix respectively.

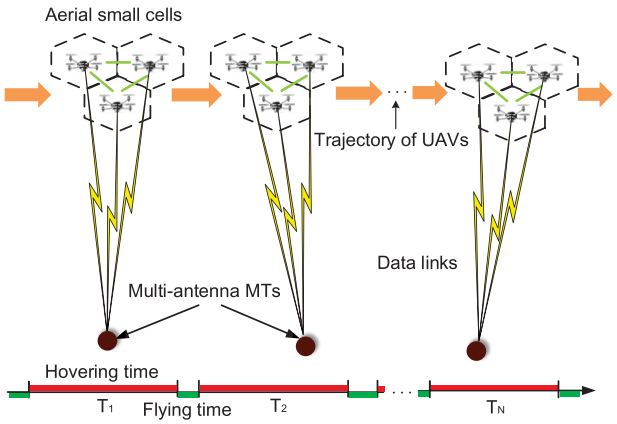

FIGURE 1. Illustration of the UAV swarm-enabled small cell network.

We consider the realistic UAV channel model [26], where the channel matrix is given by

$$\mathbf{H}_n = \mathbf{S}_n \mathbf{L}_n, \quad n = 1 \sim N. \tag{2}$$

In (2), $\mathbf{S}_n \in \mathbb{C}^{M\times K}$ whose elements are i.i.d. standard complex Gaussian random variables. These variables describe the fast fading caused by NLOS multi-path components. Besides, $\mathbf{L}_n = \text{diag}\left\{l_{n,1}, \ldots, l_{n,K}\right\} \in \mathbb{C}^{K\times K}$ is a diagonal matrix. According to [26], we have

$$l_{n,k} = d_{n,k}^{-2} 10^{-\frac{\delta_{n,k}}{10}}, \quad n = 1 \sim N,\ k = 1 \sim K \tag{3}$$

where $d_{n,k}$ denotes the distance between the n-th MT and the k-th UAV, and $\delta_{n,k}$ can be expressed as

$$\delta_{n,k} = \frac{A}{1 + ae^{-b(\theta_{n,k}-a)}} + B, \quad n = 1 \sim N,\ k = 1 \sim K \tag{4}$$

where $A = \eta_{\text{LOS}} - \eta_{\text{NLOS}}$, $B = 20\log_{10}(4\pi f/c) + \eta_{\text{NLOS}}$, η_{LOS}, η_{NLOS}, a, b are parameters related to the channel environment and assumed to be constant for N MTs, $\theta_{n,k} = \frac{180}{\pi}\arccos(h_{n,k}/d_{n,k})$ and $h_{n,k}$ denotes the height of the UAV. These parameters can be regarded as slowly-varying LOS components in the radio propagation.

We assume both the trajectory of UAVs and the locations of MTs are known prior to the flight [15], [16], [25]. Hence, we can use the position-related large-scale CSIT for EE optimization, i.e. $\mathbf{L}_n$ in (2). On the other hand, $\mathbf{S}_n$ varies fast and can not be precisely acquired by the UAVs [25]. We assume the transmitter only knows the distribution of $\mathbf{S}_n$.

It is worth noting that both the transmit power and the hovering time of UAVs are pre-scheduled prior to the flight [24]. Denoting $p_{n,k}$ as the transmit power of the k-th UAV for the n-th MT, and T_n as the hovering time of the UAV swarm for the n-th MT, we can describe the total energy consumption as [28]

$$\mathcal{E}(\mathbf{P}, \mathbf{T}) = c\sum_{n=1}^{N}\sum_{k=1}^{K} T_n \frac{p_{n,k}}{\eta_k} + P_{ind}T_{total} \tag{5}$$

where $\mathbf{P} = \{\mathbf{P}_1, \ldots, \mathbf{P}_N\}$ denotes the set of transmit power, $\mathbf{P}_n = \text{diag}\left\{p_{n,1}, \ldots, p_{n,K}\right\}$ is the diagonal power matrix, $\mathbf{T} = (T_1, \ldots, T_N)^T$ denotes the hovering time of the UAV swarm, c is the power loss coefficient, η_k describes the power amplifier efficiency of the k-th UAV, P_{ind} denotes the transmission-power-independent power consumption (e.g. the average propulsion power consumption), usually regarded as constant [25], [28], and T_{total} denotes the total hovering time. Accordingly, the total data size transmitted by the UAV swarm is written as [25]

$$\mathcal{D}(\mathbf{P}, \mathbf{T}) = \sum_{n=1}^{N} T_n \log_2 \det\left(\mathbf{I}_n + \frac{1}{\sigma^2}\mathbf{S}_n\mathbf{L}_n\mathbf{P}_n\mathbf{L}_n^H\mathbf{S}_n^H\right). \tag{6}$$

Due to the fast moving of UAVs, it is challenging to acquire the instantaneous CSIT (i.e. $\mathbf{S}_n$). Therefore, we use the *ergodic* total data size to calculate EE,

$$\eta(\mathbf{P}, \mathbf{T}) = \frac{\mathbf{E}_{\mathbf{S}}\left\{\mathcal{D}(\mathbf{P}, \mathbf{T})\right\}}{\mathcal{E}(\mathbf{P}, \mathbf{T})} \tag{7}$$

where $\eta(\mathbf{P}, \mathbf{T})$ is the EE of UAV communication, $\mathbf{E}_{\mathbf{S}}\left\{\mathcal{D}(\mathbf{P}, \mathbf{T})\right\}$ denotes the ergodic total data size, which has been averaged over all possible realizations of $\mathbf{S}$, where $\mathbf{S} = \{\mathbf{S}_1, \ldots, \mathbf{S}_N\}$ is the set of small-scale channel parameters.

In UAV networks, the optimization of EE is limited by practical constraints, such as the on-board energy of each UAV. Denoting the maximum transmit energy of the k-th UAV as E_k, the transmit energy constraints can be formulated as

$$\sum_{n=1}^{N} T_n p_{n,k} \le E_k, \quad k = 1 \sim K \tag{8}$$

where T_n and $p_{n,k}$ are defined in (5). Moreover, limited by the performance of on-board devices [1], the transmit power of UAVs is upper bounded. We can derive the power constraints of the UAVs as

$$0 \le p_{n,k} \le p_{max}, \quad n = 1 \sim N,\ k = 1 \sim K \tag{9}$$

where p_{max} denotes the maximum transmit power of a single UAV.

Another constraint that needs to be considered is the UAV hovering time, due to the limitations of the UAV flight [8], [16]. Specifically, both the total hovering time and the maximum hovering time of the UAV swarm at each MT should be considered. The constraints can be formulated as

$$\sum_{n=1}^{N} T_n \le T_{total} \tag{10}$$

$$0 \le T_n \le T_{max}, \quad n = 1 \sim N \tag{11}$$

where T_{total} denotes the total hovering time of UAVs during the flight, T_{max} denotes the maximum hovering time of UAVs when serving a MT.

Based on (5)–(11), the EE maximization problem now can be formulated as

$$\max_{\mathbf{P},\mathbf{T}} \ \eta(\mathbf{P}, \mathbf{T}) \tag{12a}$$

$$s.t.\ \sum_{n=1}^{N} T_n \le T_{total} \tag{12b}$$

$$\sum_{n=1}^{N} T_n p_{n,k} \le E_k, \quad k = 1 \sim K \tag{12c}$$

$$0 \le p_{n,k} \le p_{max}, \quad n = 1 \sim N,\ k = 1 \sim K \tag{12d}$$

$$0 \le T_n \le T_{max}, \quad n = 1 \sim N \tag{12e}$$

where the value of the parameters in (12b)–(12e) (e.g. p_{max}, E_k, etc.) are determined by the design of UAVs and the service demand of MTs [25].

It is worth noting that expectation is involved in the objective function in (12a). Moreover, $\mathbf{P}$ and $\mathbf{T}$ are coupled in (12c). These facts indicate that the problem (12) is difficult to be solved directly. In the next section, we will propose feasible simplifications and effective algorithms to solve this problem.

III. EE OPTIMIZATION SCHEME

A. PROBLEM APPROXIMATION

We utilize the techniques proposed in [25] to simplify (12). We first formulate a new objective function $\mathcal{D}_a(\mathbf{P}, \mathbf{T}, \mathbf{w})$, which can closely approximate $E_{\mathbf{S}}\{\mathcal{D}(\mathbf{P}, \mathbf{T})\}$ without expectation,

$$\mathcal{D}_a(\mathbf{P}, \mathbf{T}, \mathbf{w}) = \sum_{n=1}^{N}\sum_{k=1}^{K} T_n \log_2\left(1 + \frac{M l_{n,k}^2 p_{n,k}}{w_n \sigma^2}\right) + M\sum_{n=1}^{N} T_n\left[\log_2(w_n) - \log_2 e(1 - w_n^{-1})\right] \tag{13}$$

where $\mathbf{w} = (w_1, \ldots, w_N)^T$ is a set of slack variables,

$$w_n = 1 + \sum_{k=1}^{K} \frac{l_{n,k}^2 p_{n,k}}{\sigma^2 + M l_{n,k}^2 p_{n,k} w_n^{-1}}, \quad n = 1 \sim N. \tag{14}$$

Using (13), the original EE maximization problem is transformed to

$$\max_{\mathbf{P},\mathbf{T}}\ \eta_a(\mathbf{P}, \mathbf{T}, \mathbf{w}) \tag{15a}$$

$$s.t.\ \sum_{n=1}^{N} T_n \le T_{total} \tag{15b}$$

$$\sum_{n=1}^{N} T_n p_{n,k} \le E_k, \quad k = 1 \sim K \tag{15c}$$

$$0 \le p_{n,k} \le p_{max}, \quad n = 1 \sim N,\ k = 1 \sim K \tag{15d}$$

$$0 \le T_n \le T_{max}, \quad n = 1 \sim N \tag{15e}$$

$$w_n = 1 + \sum_{k=1}^{K} \frac{l_{n,k}^2 p_{n,k}}{\sigma^2 + M l_{n,k}^2 p_{n,k} w_n^{-1}}, \quad n = 1 \sim N \tag{15f}$$

where

$$\eta_a(\mathbf{P}, \mathbf{T}, \mathbf{w}) = \frac{\mathcal{D}_a(\mathbf{P}, \mathbf{T}, \mathbf{w})}{\mathcal{E}(\mathbf{P}, \mathbf{T})} \tag{16}$$

and the new constraint (15f) is introduced by the coupling between $\mathbf{P}$ and $\mathbf{w}$. In fact, $\mathbf{w}$ can be regarded as an implicit function with respect to $\mathbf{P}$.

B. PROBLEM DECOMPOSITION

The new problem (15) is a nonlinear fractional optimization problem, which is non-convex due to the coupling between $\mathbf{P}$ and $\mathbf{T}$. To solve this problem, we decompose (15) into two subproblems. In the first subproblem, $\mathbf{P}$ is the optimization variable and $\mathbf{T}$ is regarded as constant. Its solution is referred to as the coordinated power allocation strategy. In the second subproblem, $\mathbf{T}$ is the optimization variable and $\mathbf{P}$ is regarded as constant. Its solution is referred to as the hovering time scheduling strategy.

Denoting the iteration index as i, the two subproblems at the i-th step can be respectively formulated as

$$\max_{\mathbf{P}^i}\ \eta_a(\mathbf{P}^i, \mathbf{T}^{i-1}, \mathbf{w}^i) \tag{17a}$$

$$s.t.\ \sum_{n=1}^{N} T_n^{i-1} p_{n,k}^i \le E_k, \quad k = 1 \sim K \tag{17b}$$

$$0 \le p_{n,k}^i \le p_{max}, \quad n = 1 \sim N,\ k = 1 \sim K \tag{17c}$$

$$w_n^i = 1 + \sum_{k=1}^{K} \frac{l_{n,k}^2 p_{n,k}^i}{\sigma_m^2 + M l_{n,k}^2 p_{n,k}^i (w_n^i)^{-1}}, \quad n = 1 \sim N \tag{17d}$$

and

$$\max_{\mathbf{T}^i}\ \eta_a(\mathbf{P}^i, \mathbf{T}^i, \mathbf{w}^i) \tag{18a}$$

$$s.t.\ \sum_{n=1}^{N} T_n^i \le T_{total} \tag{18b}$$

$$\sum_{n=1}^{N} p_{n,k}^i T_n^i \le E_k, \quad k = 1 \sim K \tag{18c}$$

$$0 \le T_n^i \le T_{max}, \quad n = 1 \sim N \tag{18d}$$

The solutions to (17) and (18) will be given in Section III.C and Section III.D, respectively.

C. COORDINATED POWER ALLOCATION

In this subsection, we derive the solution to (17). Actually, (17) is a nonlinear fractional optimization problem, which is non-convex [29]. According to [30], (17) can be transformed to a convex optimization problem as

$$\max_{\mathbf{P}^i}\ \mathcal{D}_a(\mathbf{P}^i, \mathbf{T}^{i-1}, \mathbf{w}^i) - \gamma_p \mathcal{E}(\mathbf{P}^i, \mathbf{T}^{i-1}) \tag{19a}$$

$$s.t.\ \sum_{n=1}^{N} T_n^{i-1} p_{n,k}^i \le E_k, \quad k = 1 \sim K \tag{19b}$$

$$0 \le p_{n,k}^i \le p_{max}, \quad n = 1 \sim N,\ k = 1 \sim K \tag{19c}$$

$$w_n^i = 1 + \sum_{k=1}^{K} \frac{l_{n,k}^2 p_{n,k}^i}{\sigma_m^2 + M l_{n,k}^2 p_{n,k}^i (w_n^i)^{-1}}, \quad n = 1 \sim N \tag{19d}$$

where

$$\gamma_p = \frac{\mathcal{D}_a(\mathbf{P}_*^i, \mathbf{T}^{i-1}, \mathbf{w}_*^i)}{\mathcal{E}(\mathbf{P}_*^i, \mathbf{T}^{i-1})} \tag{20}$$

and $\mathbf{P}_*^i$ is the optimal solution to (17) at the i-th step, $\mathbf{T}^{i-1}$ is regarded as constant at the i-th step, $\mathbf{w}_*^i$ is derived using (19d).

However, the value of $\mathbf{P}_*^i$ cannot be obtained unless (17) is solved, which means the value of γ_p is actually unknown in (19). Hence, we propose an algorithm to find γ_p and $\mathbf{P}_*^i$ iteratively. Denoting the iteration index as j, the problem in (19) at the j-th step can be expressed as

$$\max_{\mathbf{P}^j} \ \mathcal{D}_a(\mathbf{P}^j, \mathbf{T}^{i-1}, \mathbf{w}^j) - \gamma_p^{j-1}\mathcal{E}(\mathbf{P}^j, \mathbf{T}^{i-1}) \tag{21a}$$

$$s.t. \ \sum_{n=1}^{N} T_n^{i-1} p_{n,k}^j \le E_k, \quad k = 1 \sim K \tag{21b}$$

$$0 \le p_{n,k}^j \le p_{max}, \quad n = 1 \sim N, \ k = 1 \sim K \tag{21c}$$

$$w_n^j = 1 + \sum_{k=1}^{K} \frac{l_{n,k}^2 p_{n,k}^j}{\sigma_m^2 + M l_{n,k}^2 p_{n,k}^j (w_n^j)^{-1}}. \quad n = 1 \sim N. \tag{21d}$$

This method is summarized in Algorithm 1, and the convergence can be guaranteed according to [30].

Algorithm 1 Iterative Algorithm to Solve (21)

Input: $\{E_k, k = 1 \sim K\}, p_{max}, \mathbf{T}^{i-1}$.

1: Initialization: $\epsilon = 1 \times 10^{-3}, j = 1, \gamma_p^0 = 0$;
2: Solve (21), denoting the optimal solution is $\mathbf{P}^*$, set $\mathbf{P}^1 = \mathbf{P}^*$;
3: **While** $|\mathcal{D}_a(\mathbf{P}^j, \mathbf{T}^{i-1}, \mathbf{w}^j) - \gamma_p^{j-1}\mathcal{E}(\mathbf{P}^j, \mathbf{T}^{i-1})| > \epsilon$ **do**
4: $\quad \gamma_p^j = \mathcal{D}_a(\mathbf{P}^j, \mathbf{T}^{i-1}, \mathbf{w}^j)/\mathcal{E}(\mathbf{P}^j, \mathbf{T}^{i-1})$
5: $\quad$ j = j + 1;
6: $\quad$ Solve (21), denoting the optimal solution is $\mathbf{P}^*$, set $\mathbf{P}^j = \mathbf{P}^*$;

Output: $\mathbf{P}^j$.

Although (21) is convex [27], it is computationally expensive to solve this problem directly, due to the coupling between $\mathbf{P}$ and $\mathbf{w}$ in (21d). To reduce the complexity, we substitute $\mathbf{w}$ with $\mathbf{v} = (v_1, \ldots, v_N)^T$ as

$$w_n = e^{v_n}, \quad n = 1 \sim N. \tag{22}$$

Such substitution is feasible for the reason that w_n is positive for all n according to (14). Then, (21) can be reformulated as

$$\max_{\mathbf{P}^j} \ \min_{\mathbf{v}} f(\mathbf{P}^j, \mathbf{T}^{i-1}, \mathbf{v}) \tag{23a}$$

$$s.t. \ \sum_{n=1}^{N} T_n^{i-1} p_{n,k}^j \le E_k, \quad k = 1 \sim K \tag{23b}$$

$$0 \le p_{n,k}^j \le p_{max}, \quad n = 1 \sim N, \ k = 1 \sim K \tag{23c}$$

$$v_n \ge 0, \quad n = 1 \sim N \tag{23d}$$

where

$$f(\mathbf{P}^j, \mathbf{T}^{i-1}, \mathbf{v}) = \sum_{n=1}^{N}\sum_{k=1}^{K} T_n^{i-1}\log_2\left(1 + \frac{M l_{n,k}^2 p_{n,k}^j}{e^{v_n}\sigma_m^2}\right) + M\log_2 e \sum_{n=1}^{N} T_n^{i-1}\left(v_n + e^{-v_n} - 1\right) - \gamma_p^{j-1}\mathcal{E}(\mathbf{P}^j, \mathbf{T}^{i-1}). \tag{24}$$

The equivalence between (21) and (23) can be proved on the basis of the following proposition.

Proposition 1: When $\mathbf{w}$ satisfies (14), the corresponding $\mathbf{v}$ is the extreme point of $f(\mathbf{P}^j, \mathbf{T}^{i-1}, \mathbf{v})$ with respect to $\mathbf{v}$.

Proof: We can derive the first-order derivative of $f(\mathbf{P}^j, \mathbf{T}^{i-1}, \mathbf{v})$ with respect to $\mathbf{v}$ as

$$\frac{\partial f}{\partial v_n} = \frac{M T_n^{i-1}}{\ln 2}\left(-\sum_{k=1}^{K} \frac{l_{n,k}^2 p_{n,k}^j e^{-v_n}}{\sigma_m^2 + M l_{n,k}^2 p_{n,k}^j e^{-v_n}} - e^{-v_n} + 1\right), \quad n = 1 \sim N. \tag{25}$$

Based on (25), we can find the extreme point of $f(\mathbf{P}^j, \mathbf{T}^{i-1}, \mathbf{v})$ when $\frac{\partial f}{\partial v_n} = 0$, so that we have

$$\sum_{k=1}^{K} \frac{l_{n,k}^2 p_{n,k}^j e^{-v_n}}{\sigma_m^2 + M l_{n,k}^2 p_{n,k}^j e^{-v_n}} + e^{-v_n} - 1 = 0, \quad n = 1 \sim N \tag{26}$$

which can be further rewritten as

$$e^{v_n} = 1 + \sum_{k=1}^{K} \frac{l_{n,k}^2 p_{n,k}^j}{\sigma_m^2 + M l_{n,k}^2 p_{n,k}^j e^{-v_n}}, \quad n = 1 \sim N. \tag{27}$$

Note that we have $w_n = e^{v_n}$ for $n = 1 \sim N$. Hence, (27) is equivalent to (14). □

In (24), it is easy to find that $f(\mathbf{P}^j, \mathbf{T}^{i-1}, \mathbf{v})$ is convex with respect to $\mathbf{v}$. As a result, the minimum value of $f(\mathbf{P}^j, \mathbf{T}^{i-1}, \mathbf{v})$ is achieved at the extreme point with respect to $\mathbf{v}$. Based on Proposition 1, the equivalence between (21) and (23) is proved.

Moreover, we can observe that $f(\mathbf{P}^j, \mathbf{T}^{i-1}, \mathbf{v})$ is concave with respect to $\mathbf{P}^j$. According to [31], the optimal solution is a saddle point of $f(\mathbf{P}^j, \mathbf{T}^{i-1}, \mathbf{v})$. As a result, (23) can be solved in an iterative way after being decomposed into two subproblems. Denoting the iteration index as t, the subproblems at the t-th step can be formulated as

$$\max_{\mathbf{P}^t} \ f(\mathbf{P}^t, \mathbf{T}^{i-1}, \mathbf{v}^{t-1}) \tag{28a}$$

$$s.t. \ \sum_{n=1}^{N} T_n^{i-1} p_{n,k}^t \le E_k, \quad k = 1 \sim K \tag{28b}$$

$$0 \le p_{n,k}^t \le p_{max}, \quad n = 1 \sim N, \ k = 1 \sim K \tag{28c}$$

and

$$\min_{\mathbf{v}^t} \ f(\mathbf{P}^t, \mathbf{T}^{i-1}, \mathbf{v}^t) \tag{29a}$$

$$s.t. \ v_n^t \ge 0, \quad n = 1 \sim N \tag{29b}$$

Algorithm 2 Iterative Algorithm to Solve (23)

Input: $\{E_k, k = 1 \sim K\}$, p_{max}, $\mathbf{T}^{i-1}$, γ_p^{j-1}.

1: Initialization: $\epsilon = 1 \times 10^{-3}$, $t = 1$, $\mathbf{P}^0 = \mathbf{0}$, $\mathbf{v}^0 = \mathbf{0}$;
2: Solve (28), denoting the optimal solution is $\mathbf{P}^*$, set $\mathbf{P}^1 = \mathbf{P}^*$;
3: Solve (29), denoting the optimal solution is $\mathbf{v}^*$, set $\mathbf{v}^1 = \mathbf{v}^*$;
4: **While** $|f(\mathbf{P}^t, \mathbf{T}^{i-1}, \mathbf{v}^t) - f(\mathbf{P}^{t-1}, \mathbf{T}^{i-1}, \mathbf{v}^{t-1})| > \epsilon$ **do**
5: $\quad$ t = t + 1;
6: $\quad$ Solve (28), denoting the optimal solution is $\mathbf{P}^*$, set $\mathbf{P}^t = \mathbf{P}^*$;
7: $\quad$ Solve (29), denoting the optimal solution is $\mathbf{v}^*$, set $\mathbf{v}^t = \mathbf{v}^*$;

Output: $\mathbf{P}^t$.

where $\mathbf{T}^{i-1}$ and γ_p^{j-1} in (24) are regarded as constants. This scheme is summarized in Algorithm 2, and its convergence is guaranteed according to [27, Theorem 2]. Recalling that the objective function is convex with respect to $\mathbf{v}^t$ and concave with respect to $\mathbf{P}^t$, both (28) and (29) can be solved using conventional convex optimization tools [29].

D. HOVERING TIME SCHEDULING

As (18) is similar to (17), it can be solved following the same line of reasoning as Algorithm 1. However, the computational complexity of the iterative algorithm is large. To address this problem, we propose a scheme to solve (18) directly.

It is easy to find that (18) is a linear fractional optimization problem with linear constraints. According to [29, Section 4.3.2], the optimal solution to a linear fractional optimization problem can be derived based on the solution to a linear optimization problem, after a slack variable is introduced. The linear optimization problem is written as

$$\max_{\mathbf{T}^i, z} \ \mathcal{D}_a(\mathbf{P}^i, \mathbf{T}^i, \mathbf{w}^i) \tag{30a}$$

$$s.t. \ \sum_{n=1}^{N}\sum_{k=1}^{K} \frac{p_{n,k}^i}{\eta_k} T_n^i + P_{ind} T_{total} z = 1 \tag{30b}$$

$$\sum_{n=1}^{N} T_n^i - T_{total} z \le 0 \tag{30c}$$

$$\sum_{n=1}^{N} p_{n,k}^i T_n^i - E_k z \le 0, \quad k = 1 \sim K \tag{30d}$$

$$T_n^i - T_{max} z \le 0, \quad n = 1 \sim N \tag{30e}$$

$$z \ge 0 \tag{30f}$$

$$T_n^i \ge 0, \quad n = 1 \sim N \tag{30g}$$

where $\mathbf{P}^i$ and $\mathbf{w}^i$ can be regarded as constants which satisfy (14), and z is the introduced slack variable. According to [29], the solution to (18) can be derived based on the solution to (30).

Before discussing the relationship between (18) and (30), we firstly introduce a property of (30).

Proposition 2: Denoting the optimal solution to (30) as $(\mathbf{T}^*, z^*)$, we have $z^* > 0$.

Proof: Based on (30g), we only need to prove that $z^* \neq 0$. If $z^* = 0$, we will have $\mathbf{T}^* = \mathbf{0}$ according to (30e) and (30f). Note that $(\mathbf{T}^*, z^*)$ must satisfy the constraint in (30b). If we substitute $z^* = 0$ and $\mathbf{T}^* = \mathbf{0}$ into (30b), we will have $0 = 1$, which is contradict to the original assumption that $z^* = 0$. As a result, $z^* > 0$ is given. □

The conclusion of Proposition 2 shows that we can calculate $1/z^*$ without any discussions, because the value of z^* is always positive. Based on *Proposition 2*, we can give the optimal solution to (18), which will be shown in the following proposition.

Proposition 3: The optimal solution to (18) is $\mathbf{T}^*/z^*$.

Proof: Firstly, we claim that $\mathbf{T}^*/z^*$ is a feasible solution to (18). The reason is that according to (30c)–(30g), (18b)–(18d) are satisfied by $\mathbf{T}^*/z^*$ obviously, so that $\mathbf{T}^*/z^*$ is a feasible solution to (18).

Denoting the optimal solution to (18) as $\hat{\mathbf{T}}$, we define $\hat{z} = 1/\mathcal{E}(\mathbf{P}^i, \hat{\mathbf{T}})$. Then, substituting $(\hat{\mathbf{T}}\hat{z}, \hat{z})$ into (30), we can find that $(\hat{\mathbf{T}}\hat{z}, \hat{z})$ is a feasible solution to (30). Due to the optimality of $\mathbf{T}^*$ in (30), we have

$$\mathcal{D}_a(\mathbf{P}^i, \mathbf{T}^*, \mathbf{w}^i) \ge \mathcal{D}_a(\mathbf{P}^i, \hat{\mathbf{T}}\hat{z}, \mathbf{w}^i). \tag{31}$$

As $(\hat{\mathbf{T}}\hat{z}, \hat{z})$ is a feasible solution to (30) which satisfies (30b), we have

$$\begin{aligned}\mathcal{D}_a(\mathbf{P}^i, \hat{\mathbf{T}}\hat{z}, \mathbf{w}^i) &= \frac{\mathcal{D}_a(\mathbf{P}^i, \hat{\mathbf{T}}\hat{z}, \mathbf{w}^i)}{c\sum_{n=1}^{N}\sum_{k=1}^{K} \hat{T}_n \hat{z} \frac{p_{n,k}}{\eta_k} + P_{ind} T_{total} \hat{z}} \\ &= \frac{\mathcal{D}_a(\mathbf{P}^i, \hat{\mathbf{T}}, \mathbf{w}^i)}{\mathcal{E}(\mathbf{P}^i, \hat{\mathbf{T}})}\end{aligned} \tag{32}$$

and

$$\begin{aligned}\mathcal{D}_a(\mathbf{P}^i, \mathbf{T}^*, \mathbf{w}^i) &= \frac{\mathcal{D}_a(\mathbf{P}^i, \mathbf{T}^*, \mathbf{w}^i)}{c\sum_{n=1}^{N}\sum_{k=1}^{K} T_n^* \frac{p_{n,k}}{\eta_k} + P_{ind} T_{total} z^*} \\ &= \frac{\mathcal{D}_a(\mathbf{P}^i, \mathbf{T}^*/z^*, \mathbf{w}^i)}{\mathcal{E}(\mathbf{P}^i, \mathbf{T}^*/z^*)}\end{aligned} \tag{33}$$

because $(\mathbf{T}^*, z^*)$ also satisfies (30b). Hence, we have

$$\frac{\mathcal{D}_a(\mathbf{P}^i, \mathbf{T}^*/z^*, \mathbf{w}^i)}{\mathcal{E}(\mathbf{P}^i, \mathbf{T}^*/z^*)} \ge \frac{\mathcal{D}_a(\mathbf{P}^i, \hat{\mathbf{T}}, \mathbf{w}^i)}{\mathcal{E}(\mathbf{P}^i, \hat{\mathbf{T}})} \tag{34}$$

according to (31), which means $\mathbf{T}^*/z^*$ is the optimal solution to (18). □

Using *Proposition 2* and *Proposition 3*, we can derive the optimal solution to (18) after the optimal solution to (30) is given. As shown in (13) and (30a)–(30g), (30) is a linear optimization problem. Such problem can be directly solved using conventional linear optimization tools [29].

Based on the solutions to (23) and (30), we propose an iterative algorithm to solve (15), which is summarized in Algorithm 3. The proof of its convergence is provided in Appendix A. Using Algorithm 3, the original EE maximization problem can be efficiently solved.

Algorithm 3 Proposed EE Optimization Algorithm

Input: $\{E_k, k = 1 \sim K\}, T_{total}, p_{max}, T_{max}$

1: Initialization: $\epsilon = 1 \times 10^{-4}$, $i = 1$, $\mathbf{T}^0 = (T_{total}/N)\mathbf{1}$, $\mathbf{P}^0 = \mathbf{0}$;
2: Solve (17), denoting the optimal solution is $\mathbf{P}^*$, set $\mathbf{P}^1 = \mathbf{P}^*$;
3: **While** $|\eta_a(\mathbf{P}^i, \mathbf{T}^{i-1}, \mathbf{w}^i) - \eta_a(\mathbf{P}^{i-1}, \mathbf{T}^{i-1}, \mathbf{w}^{i-1})| > \epsilon$ **do**
4: Solve (18), denoting the optimal solution is $\mathbf{T}^*$, set $\mathbf{T}^i = \mathbf{T}^*$;
5: i = i + 1;
6: Solve (17), denoting the optimal solution is $\mathbf{P}^*$, set $\mathbf{P}^i = \mathbf{P}^*$;

Output: $\mathbf{P}^i$, $\mathbf{T}^i$.

IV. SIMULATION RESULTS

In this section, we evaluate the proposed EE maximization scheme through simulations. We assume each MT equips with $M = 6$ receive antennas, the number of UAVs in a swarm is set as $K = 6$ and the number of MTs is set as $N = 10$. For the channel parameters, we set $f = 2$ GHz, $c = 3 \times 10^8$ m/s, $\eta_{\text{LOS}} = 0.1$, $\eta_{\text{NLOS}} = 21$, $a = 5.0188$, $b = 0.3511$ according to [26], $d_{n,k}$ and $h_{n,k}$ are randomly generated but are fixed in each realization. The noise power is set as $\sigma^2 = -107$ dBm. Regarding the total energy in (5), we set $c = 2.63$, $\eta_k = 0.08$ for $k = 1 \sim K$, $P_{ind} = 20$ dB [28]. We set the power limit of a UAV as $p_{max} = 300$ mW [25]. Without loss of fairness, we assume the UAVs have the same E_k for $k = 1 \sim K$, and the sum of E_k is denoted as E_{total}.

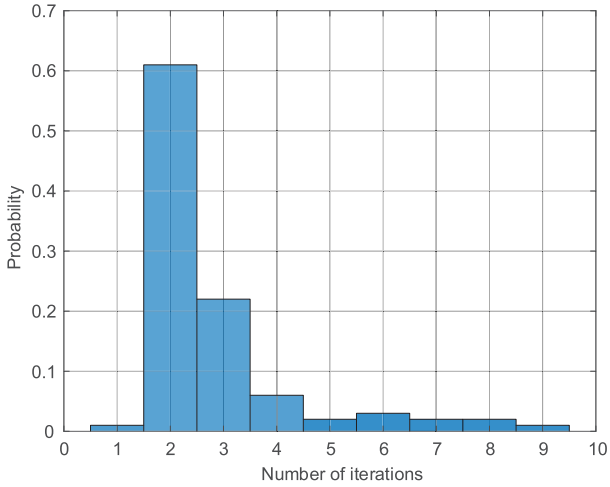

FIGURE 2. Convergence performance of the proposed EE optimization algorithm, shown by the distribution of iteration times.

In Fig. 2, we evaluate the convergence performance of the proposed EE optimization algorithm. In this simulation, we set $T_{total} = 100$ s, $T_{max} = 15$ s and the total transmit energy (i.e. E_{total}) is set as 30 J. These parameters are applied for all the subsequent simulations, unless otherwise specified. The proposed algorithm has been tested over 100 snapshots, where for every snapshot the positions of the UAVs and the users are randomly and independently generated. According to the results, the algorithm needs 2.77 iterations on average to converge. To demonstrate the convergence performance, we show the distribution of the iteration times by the histogram. The result shows that the convergence performance of the proposed algorithm can be guaranteed for practical UAV swarm-enabled small cell networks.

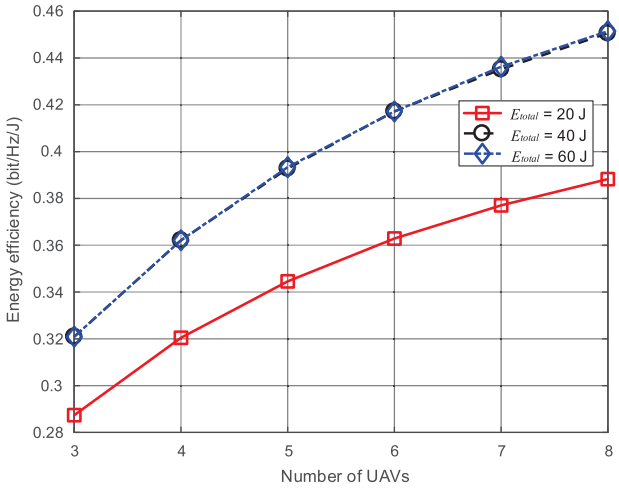

FIGURE 3. The EE of communication when the total transmit energy of UAVs is different, varying with the number of UAVs.

In Fig. 3, we discuss the influence of UAV swarm size on the EE performance. It is observed that when the swarm size increases (while keeping the total transmit energy fixed), a better EE performance is achieved. One reason for this phenomenon is that a higher diversity gain can be obtained with more UAVs in a swarm. Moreover, the coordination of aerial small cells is more flexible with larger swarm size, which leads to a better performance of EE. Besides, the EE performance cannot be infinitely improved by increasing the UAV swarm size, because the transmit energy of each UAV is less with larger swarm size. We further observe that the EE is saturated at high transmit energy. The reason is that the transmit power of most UAVs will reach the upper bound in this case. Hence, the EE can hardly be further improved by increasing the transmit energy.

In Fig. 4, we investigate the relationship between the maximum hovering time of a single UAV and the EE. We can observe that the EE can be effectively improved if the UAVs are allowed to hover more time above the MTs. The reason is that the feasible region of the EE maximization problem becomes larger when the maximum hovering time increases, so that higher EE can be achieved after the EE maximization problem is solved. We can further observe that the proposed algorithm tends to allocate more hovering time to the MTs with better channel conditions to maximize the EE, which means less MTs are served in practice by UAVs with larger maximum hovering time. This result indicates that there

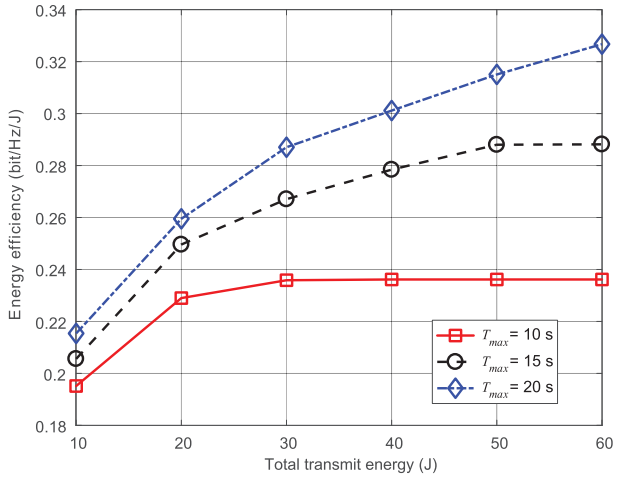

FIGURE 4. The EE of communication with different maximum hovering time of a single UAV, varying with the total transmit energy of UAVs.

exists a tradeoff between the user number and EE in UAV swarm-enabled small cell networks.

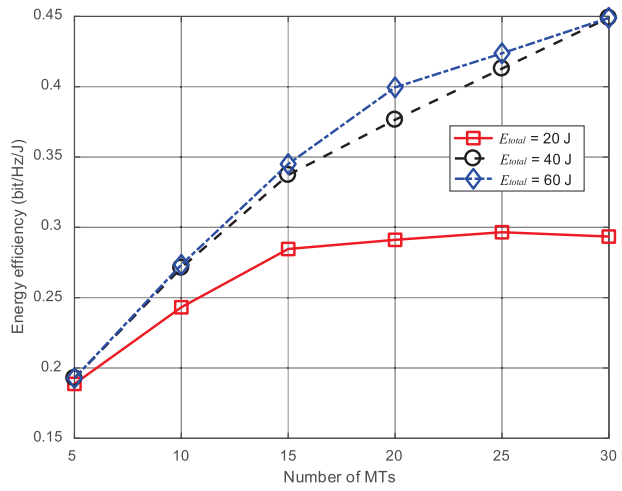

FIGURE 5. The EE of communication when the total transmit energy of UAVs is different, varying with the number of MTs.

In Fig. 5, we further discuss the influence of user number on the EE. It is observed that the increasing number of MTs has a positive influence on the EE performance, for the reason that more MTs with better channel condition can be chosen to serve by UAVs. In other words, after the MTs are scheduled by the proposed algorithm, the MTs with bad channel condition are not served by UAVs. This result shows that the tradeoff between the user number and EE actually exists in UAV swarm-enabled small cell networks when the total transmit energy is fixed, as analyzed in Fig. 4. Furthermore, we can observe that increasing the total transmit energy is a better way to improve the EE performance with larger number of MTs, which implies that the transmit energy is a critical bottleneck for UAV swarm-enabled small cell networks.

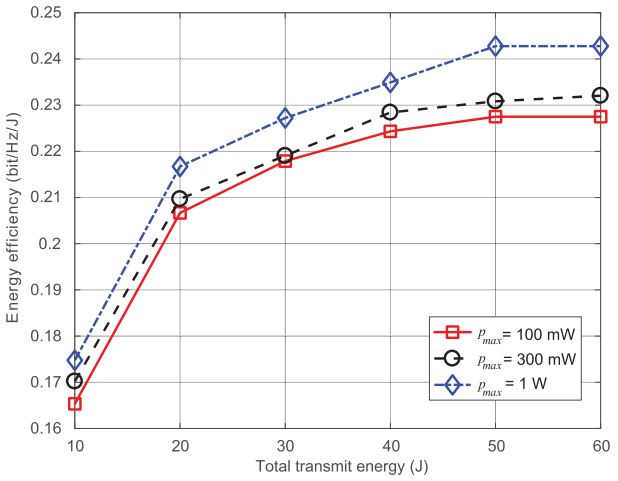

FIGURE 6. The EE of communication with different power limit of UAVs, varying with the total transmit energy of UAVs.

In Fig. 6, the influence of power limit on the EE performance is evaluated. It is observed that the EE increases with larger power limit. Similar to the analysis in Fig. 4, the reason for this phenomenon is that higher EE can be achieved when the feasible region of the EE maximization problem is larger. We can also observe that the curves are close to each other when the maximum transmit power is 100 mW and 300 mW. This is because part of performance loss can be compensated by hovering time scheduling when the transmit power is low. Such performance loss is hard to be compensated by hovering time scheduling when the transmit power is high, because the total transmit energy is limited.

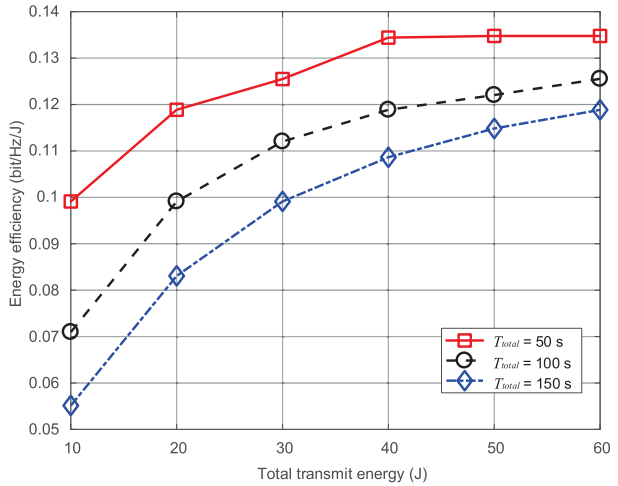

FIGURE 7. The EE of communication with different total hovering time of UAVs, varying with the total transmit energy of UAVs.

In Fig. 7, we show the EE versus the total transmit energy for different total hovering time. The maximum hovering time of a single UAV is set proportional to the total hovering time to control variables, which are 7.5 s, 15 s

and 22.5 s respectively. As shown by the simulation results, reducing the total hovering time leads to higher EE. The reason is that the transmit power of UAVs is generally higher when the total transmit energy is consumed in a shorter time. In this case, higher EE is achieved due to higher transmit power.

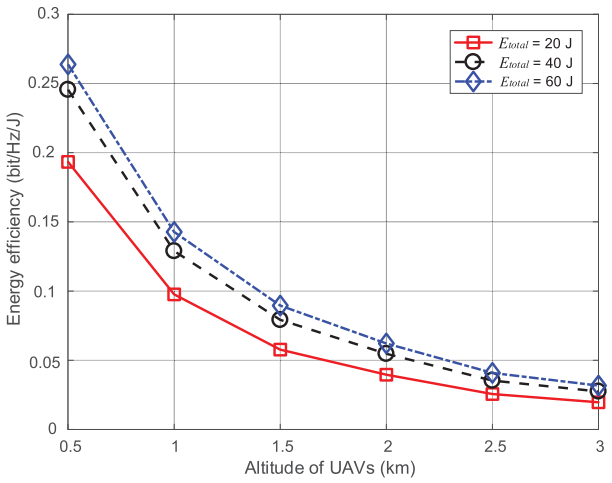

FIGURE 8. The EE of communication when the total transmit energy of UAVs is different, varying with the altitude of UAVs.

In Fig. 8, we demonstrate the EE with varying altitudes of UAVs. Specifically, we set $h_{n,k} = h_U + 300\phi_{n,k}$, where $\phi_{n,k}$ are uniformly distributed variables in the range of [0, 1] m, and h_U changes from 0.5 km to 3 km. As demonstrated by the curves, we can observe that a higher EE can be achieved and the EE can be better improved by increasing the transmit power, when the altitude of UAVs is lower. The reason is that channel fading is less severe when the UAVs are hovering at a lower altitude. In this case, the total data size can become larger when the total energy consumption remains unchanged, which means a better performance can be achieved. On the other hand, the low altitude of UAVs results in a limited coverage area. These results imply that there exists a tradeoff between the coverage area and EE in UAV swarm-enabled small cell networks.

In Fig. 9, we compare the proposed algorithm with the conventional algorithm, which allocates the transmit power and hovering time of UAVs equally between the MTs, and the algorithm in [25]. We can observe that the EE increases with the total transmit energy, as a larger transmit energy can provide higher degrees of freedom for EE optimization. More importantly, it is shown that the proposed algorithm outperforms other schemes on the regime of transmit energy. When the transmit energy is lower than 30 J, the proposed algorithm has a similar performance to the algorithm in [25]. The reason is that the total energy consumption is nearly a constant when the transmit energy is much lower than the transmission-energy-independent energy consumption. In this case, the optimization of total data size is similar to the optimization of EE. When the transmit energy becomes

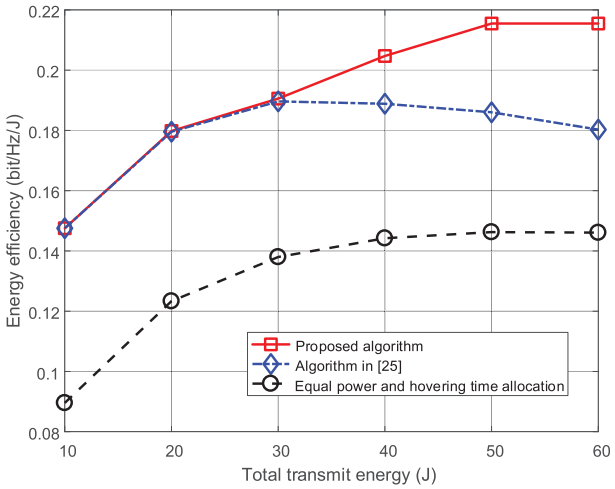

FIGURE 9. The EE of communication using different optimization algorithms, varying with the total transmit energy of UAVs.

higher, the gap between the proposed algorithm and other algorithms becomes larger. The results indicate that optimizing the EE is important for the UAV swarm-enabled small cell network, especially with high transmit energy.

V. CONCLUSION

In this paper, we have investigated the optimization of EE for UAV swarm-enabled small cell networks with large-scale CSIT, considering the coordination of aerial small cells under energy constraints. The EE maximization problem has been formulated, which is a non-convex fractional optimization problem and hard to be solved directly. We have decomposed it into two subproblems, which can be efficiently solved by the proposed iterative algorithm. Simulation results have demonstrated that it is valuable to jointly consider the coordination of aerial small cells and the large-scale CSIT when optimizing the EE for UAV swarm-enabled small cell networks.

APPENDIX
PROOF OF THE CONVERGENCE OF ALGORITHM 3

Assuming that $\mathbf{P}^{i-1}$ and $\mathbf{T}^{i-1}$ are solutions to (17) and (18) at the $(i-1)$-th step. After we solve (17), we have $\mathbf{P}^i$ as the optimal solution, which satisfies

$$\eta_a(\mathbf{P}^i, \mathbf{T}^{i-1}, \mathbf{w}^i) \geq \eta_a(\mathbf{P}^{i-1}, \mathbf{T}^{i-1}, \mathbf{w}^{i-1}). \quad \text{(A.1)}$$

Then after (18) is solved at the i-th step, we have $\mathbf{T}^i$ as the optimal solution, which satisfies

$$\eta_a(\mathbf{P}^i, \mathbf{T}^i, \mathbf{w}^i) \geq \eta_a(\mathbf{P}^i, \mathbf{T}^{i-1}, \mathbf{w}^i). \quad \text{(A.2)}$$

According to (A.1) and (A.2), we have

$$\eta_a(\mathbf{P}^i, \mathbf{T}^i, \mathbf{w}^i) \geq \eta_a(\mathbf{P}^{i-1}, \mathbf{T}^{i-1}, \mathbf{w}^{i-1}) \quad \text{(A.3)}$$

which means the objective function of (15) keeps increasing at every step of the iteration, and it is upper bounded by the

given resources. As a result, Algorithm 3 is guaranteed to converge.

REFERENCES

[1] S. Hayat, E. Yanmaz, and R. Muzaffar, "Survey on unmanned aerial vehicle networks for civil applications: A communications viewpoint," *IEEE Commun. Surveys Tuts.*, vol. 18, no. 4, pp. 2624–2661, 4th Quart., 2016.

[2] B. Li, Z. Fei, and Y. Zhang, "UAV communications for 5G and beyond: Recent advances and future trends," *IEEE Intern. Things J.*, vol. 6, no. 2, pp. 2241–2263, Apr. 2019. doi: 10.1109/JIOT.2018.2887086.

[3] L. Gupta, R. Jain, and G. Vaszkun, "Survey of important issues in UAV communication networks," *IEEE Commun. Surveys Tuts.*, vol. 18, no. 2, pp. 1123–1152, 2nd Quart., 2016.

[4] T. Qi, W. Feng, and Y. Wang, "Outage performance of non-orthogonal multiple access based unmanned aerial vehicles satellite networks," *China Commu.*, vol. 15, no. 5, pp. 1–8, May 2018.

[5] Z. Yuan, J. Jin, L. Sun, K.-W. Chin, and G.-M. Muntean, "Ultra-reliable IoT communications with UAVs: A swarm use case," *IEEE Commun. Mag.*, vol. 56, no. 12, pp. 90–96, Dec. 2018.

[6] Y. Zeng, R. Zhang, and T. J. Lim, "Wireless communications with unmanned aerial vehicles: Opportunities and challenges," *IEEE Commun. Mag.*, vol. 54, no. 5, pp. 36–42, May 2016.

[7] Y. Zeng and R. Zhang, "Energy-efficient UAV communication with trajectory optimization," *IEEE Trans. Wireless Commun.*, vol. 16, no. 6, pp. 3747–3760, Jun. 2017.

[8] M. Mozaffari, W. Saad, M. Bennis, and M. Debbah, "Mobile unmanned aerial vehicles (UAVs) for energy-efficient Internet of Things communications," *IEEE Trans. Wireless Commun.*, vol. 16, no. 11, pp. 7574–7589, Nov. 2017.

[9] C. H. Liu, Z. Chen, J. Tang, J. Xu, and C. Piao, "Energy-efficient UAV control for effective and fair communication coverage: A deep reinforcement learning approach," *IEEE J. Sel. Areas Commun.*, vol. 36, no. 9, pp. 2059–2070, Sep. 2018.

[10] Q. Song and F. Zheng, "Energy efficient multi-antenna UAV-enabled mobile relay," *China Commun.*, vol. 15, no. 5, pp. 44–50, May 2018.

[11] Z. Zhou, C. Zhang, C. Xu, F. Xiong, Y. Zhang, and T. Umer, "Energy-efficient industrial Internet of UAVs for power line inspection in smart grid," *IEEE Trans. Ind. Informat.*, vol. 14, no. 6, pp. 2705–2714, Jun. 2018.

[12] M. B. Ghorbel, H. Ghazzai, A. Kadri, M. J. Hossain, and H. Menouar, "An energy efficient overlay cognitive radio approach in UAV-based communication," in *Proc. IEEE GLOBECOM*, Abu Dhabi, UAE, Dec. 2018, pp. 1–6.

[13] H. Shakhatreh, A. Khreishah, J. Chakareski, H. B. Salameh, and I. Khalil, "On the continuous coverage problem for a swarm of UAVs," in *Proc. IEEE 37th Sarnoff Symp.*, Newark, NJ, USA, Sep. 2016, pp. 130–135.

[14] L. Ruan, J. Wang, J. Chen, Y. Xu, Y. Yang, H. Jiang, Y. Zhang, and Y. Xu, "Energy-efficient multi-UAV coverage deployment in UAV networks: A game-theoretic framework," *China Commun.*, vol. 15, no. 10, pp. 194–209, Oct. 2018.

[15] M. Monwar, O. Semiari, and W. Saad, "Optimized path planning for inspection by unmanned aerial vehicles swarm with energy constraints," in *Proc. IEEE GLOBECOM*, Abu Dhabi, UAE, Dec. 2018, pp. 1–6.

[16] H. Ghazzai, M. B. Ghorbel, A. Kassler, and J. Hossain, "Trajectory optimization for cooperative dual-band UAV swarms," in *Proc. IEEE GLOBECOM*, Abu Dhabi, UAE, Dec. 2018, pp. 1–7.

[17] M. Chen, F. Dai, H. Wang, and L. Lei, "DFM: A distributed flocking model for UAV swarm networks," *IEEE Access*, vol. 6, pp. 69141–69150, 2018.

[18] Q. Zhang, M. Jiang, Z. Feng, W. Li, W. Zhang, and M. Pan, "IoT enabled UAV: Network architecture and routing algorithm," *IEEE Intern. Things J.*, vol. 6, no. 2, pp. 3727–3742, Apr. 2019. doi: 10.1109/JIOT.2018.2890428.

[19] R. K. Patra and P. Muthuchidambaranathan, "Optimisation of spectrum and energy efficiency in UAV-enabled mobile relaying using bisection and PSO method," in *Proc. IEEE I2CT*, Pune, India, Apr. 2018, pp. 1–7.

[20] A. M. Koushik, F. Hu, and S. Kumar, "Deep Q-Learning based node positioning for throughput-optimal communications in dynamic UAV swarm network," *IEEE Trans. Cognit. Commun. Netw.*, to be published. doi: 10.1109/TCCN.2019.2907520.

[21] N. Lu, Y. Zhou, C. Shi, N. Cheng, L. Cai, and B. Li, "Planning while flying: A measurement-aided dynamic planning of drone small cells," *IEEE Internet Things J.*, vol. 6, no. 2, pp. 2693–2705, Apr. 2019.

[22] S.-F. Chou, Y.-J. Yu, A.-C. Pang, and T.-A. Lin, "Energy-aware 3D aerial small-cell deployment over next generation cellular networks," in *Proc. IEEE VTC-Spring*, Porto, Portugal, Jun. 2018, pp. 1–5.

[23] A. A. Khuwaja, G. Zheng, Y. Chen, and W. Feng, "Optimum deployment of multiple UAVs for coverage area maximization in the presence of co-channel interference," *IEEE Access*, vol. 7, pp. 85203–85212, 2019.

[24] M. Mozaffari, W. Saad, M. Bennis, and M. Debbah, "Wireless communication using unmanned aerial vehicles (UAVs): Optimal transport theory for hover time optimization," *IEEE Trans. Wireless Commun.*, vol. 16, no. 12, pp. 8052–8066, Dec. 2017.

[25] W. Feng, J. Wang, Y. Chen, X. Wang, N. Ge, and J. Lu, "UAV-aided MIMO communications for 5G Internet of Things," *IEEE Internet Things J.*, vol. 6, no. 2, pp. 1731–1740, Apr. 2019.

[26] Y. Chen, W. Feng, and G. Zheng, "Optimum placement of UAV as relays," *IEEE Commun. Lett.*, vol. 22, no. 2, pp. 248–251, Feb. 2018.

[27] W. Feng, Y. Wang, N. Ge, J. Lu, and J. Zhang, "Virtual MIMO in multi-cell distributed antenna systems: Coordinated transmissions with large-scale CSIT," *IEEE J. Sel. Areas Commun.*, vol. 31, no. 10, pp. 2067–2081, Oct. 2013.

[28] J. Joung, Y. K. Chia, and S. Sun, "Energy-efficient, large-scale distributed-antenna system (L-DAS) for multiple users," *IEEE J. Sel. Topics Signal Process.*, vol. 8, no. 5, pp. 954–965, Oct. 2014.

[29] S. Boyd and L. Vandenberghe, *Convex Optimization*. Cambridge, U.K.: Cambridge Univ. Press, 2004.

[30] W. Dinkelbach, "On nonlinear fractional programming," *Manage. Sci.*, vol. 13, no. 7, pp. 492–498, Mar. 1967.

[31] W. Murray and M. L. Overton, "A projected Lagrangian algorithm for nonlinear minimax optimization," *SIAM J. Sci. Stat. Comput.*, vol. 1, no. 3, pp. 345–370, Sep. 1980.

CHENGXIAO LIU received the B.S. degree from the Department of Electronic Engineering, Tsinghua University, Beijing, China, in 2017, where he is currently pursuing the Ph.D. degree. His research interests include maritime communications, hybrid satellite-terrestrial networks, and UAV communications.

WEI FENG (S'06–M'10–SM'19) received the B.S. and Ph.D. degrees (Hons.) from the Department of Electronic Engineering, Tsinghua University, Beijing, China, in 2005 and 2010, respectively, where he is currently an Associate Professor. He is also with the Beijing National Research Center for Information Science and Technology and the Peng Cheng Laboratory. His research interests include maritime broadband communication networks, large-scale distributed antenna systems, and coordinated satellite-UAV-terrestrial networks. He has received the Outstanding Ph.D. Graduate of Tsinghua University Award, in 2010, the IEEE WCSP Best Paper Award, in 2013, the First Prize of Science and Technology Award of China Institute of Communications, in 2015, the IEEE WCSP Best Paper Award, in 2015, the Second Prize of National Technological Invention Award of China, in 2016, and the IEEE WOCC Best Paper Award, in 2019. He currently serves as an Assistant to the Editor-in-Chief of China Communications, an Editor of the IEEE Transactions on Cognitive Communications and Networking, and an Associate Editor of IEEE Access.

JUE WANG (S'10–M'14) received the B.S. degree in communications engineering from Nanjing University, Nanjing, China, in 2006, and the M.S. and Ph.D. degrees from the National Communications Research Laboratory, Southeast University, Nanjing, China, in 2009 and 2014, respectively. From 2014 to 2016, he was with the Singapore University of Technology and Design as a Postdoctoral Research Fellow. He is currently with the School of Electronic and Information Engineering, Nantong University, Nantong, China. His research interests include MIMO wireless communications, multiuser transmission, MIMO channel modeling, massive MIMO systems, and physical layer security. He has served as a Technical Program Committee Member for a number of the IEEE conferences and a Reviewer for the various IEEE journals. He was awarded as an Exemplary Reviewer of the IEEE TRANSACTIONS ON COMMUNICATIONS, in 2014.

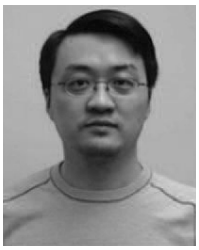

YUNFEI CHEN (S'02–M'06–SM'10) received the B.E. and M.E. degrees in electronic engineering from Shanghai Jiao Tong University, China, in 1998 and 2001, respectively, and the Ph.D. degree from the University of Alberta, Canada, in 2006. He is currently with the School of Engineering, University of Warwick, Coventry, U.K. His research interests include energy harvesting, wireless relaying and general performance analysis, and design of wireless systems.

NING GE (M'97) received the B.S. and Ph.D. degrees from Tsinghua University, China, in 1993 and 1997, respectively. From 1998 to 2000, he worked on the development of ATM switch fabric ASIC, ADC Telecommunications, Dallas, TX, USA. Since 2000, he has been with the Department of Electronics Engineering, Tsinghua University. He is currently a Professor and the Director of the Communication Institute. He has published more than 100 articles. His current interests include communication ASIC design, short range wireless communication, and wireless communications. He is also a Senior Member of CIC and CIE.